Shear Zones and Wall Slip in the Capillary Flow of Concentrated Colloidal Suspensions

Lucio Isa, Rut Besseling, and Wilson C K Poon

SUPA & School of Physics, The University of Edinburgh, James Clerk Maxwell Building, The Kings Buildings, Mayfield Road, Edinburgh EH9 3JZ, United Kingdom

(Received 28 February 2007; published 10 May 2007)

We image the flow of a nearly random close packed, hard-sphere colloidal suspension (a ''paste'') in a square capillary using confocal microscopy. The flow consists of a ''plug'' in the center while shear occurs localized adjacent to the channel walls, reminiscent of yield-stress fluid behavior. However, the observed scaling of the velocity profiles with the flow rate strongly contrasts yield-stress fluid predictions. Instead, the velocity profiles can be captured by a theory of stress fluctuations originally developed for chute flow of dry granular media. We verified this both for smooth and rough walls.

DOI: 10.1103/PhysRevLett.98.198305 PACS numbers: 83.80.Hj, 83.50.Ha, 83.60.La

Understanding the deformation and flow, or rheology, of complex fluids in terms of their constituents (colloids, polymers, or surfactants) poses deep fundamental challenges, and has wide applications [1]. Experimental complex fluid rheology typically starts in a rheometer, in which stresses and strains are applied and measured in well-defined, ''rheometric'' geometries (''cone-plate'', etc.). Translating rheometer data to more complex flows is nontrivial, but well developed in polymers (see, e.g., [2]).

The understanding of colloidal flows lags considerably behind and despite their equal practical importance [3,4], studies on model systems have been carried out only recently [5]. Compared to polymers, colloids pose some unique challenges. Concentrated suspensions (''pastes'') are generally nonergodic (or ''glassy''), so that *any* flow involves nonlinearities (e.g., yielding [6,7] or shear thickening [8,9]). Moreover, specific geometries in applications may involve dimensions comparable to single particles and lead to confinement effects, such as in microfluidics [10]. The most quantitative theory for quiescent colloidal glasses, mode coupling theory, has only recently been extended to deal with simple shear [11].

Here we present an experimental study of the flow of a hard-sphere suspension at nearly random close packing, a paste, in a 20-particle-wide square capillary. Pastes are ubiquitous in industry, where their unique rheology presents many challenges and opportunities [4]. The simplicity of the geometry is appealing from the fundamental perspective. It also makes direct contact with microfluidic applications [10]. Using fast confocal microscopy, we tracked the motion of individual colloids and measured the velocity profiles in channels with both smooth and rough walls. Despite the colloidal nature of our suspension, we find significant similarities with granular flow, itself of wide applied [12] and fundamental [13] interest.

We used sterically stabilized polymethylmethacrylate (PMMA) spheres of diameter $\bar{D} = 2.6 \pm 0.1$ μm (from confocal microscopy) fluorescently labeled with nitrobenzoxadiazole, and suspended in a mixture of cycloheptylbromide and mixed decalin (viscosity 2.6 mPa · s) for buoyancy matching at room temperature $T = T_r$. Their Brownian time is $\tau_B = \bar{D}^2/24D_0 \simeq 4.4$ s with D_0 the bare diffusion coefficient.

A dense suspension (volume fraction $\phi \gtrsim 0.63$, from confocal microscopy) was obtained by centrifuging (at $T > T_r$ to remove buoyancy matching). A constant pressure gradient, ∇p, is applied to drive the suspension into a square borosilicate glass micro-channel (Vitrocom Ltd; side $2a = 50$ μm) [14], whose inner walls were either untreated and smooth, or coated with a disordered monolayer of colloids and thus rough on the particle level. The coating particles, sightly larger ($\bar{D}_{\text{coat}} = 2.8$ μm) and more polydisperse PMMA spheres (inset, Fig. 5), were applied by filling with a dilute suspension and attached by heating in a vacuum oven (110 °C).

The flow (along x) across the full width of the channel ($|y| \leq a$) was imaged with a Visitech VTeye confocal scanner in a Nikkon TE Eclipse 300 inverted microscope. We collected 44 μm × 58 μm images (107 frames per second) at depths $-a < z < +0.2a$ ($z = -a$ is the lower surface). From the two-dimensional images, we located particles with a resolution δx, $\delta y \simeq 50$ nm [15]. A key step for correct tracking is to follow colloids in a ''comoving'' frame [14]. This involves removing from the ''raw'' coordinates the advective motion $\Delta x(\bar{y})$, which is obtained as the x shift that maximizes the cross correlation between image strips around $\bar{y}$ in successive frames. From time-dependent coordinates (restored in the lab frame), we obtained particle velocities [16]. After start-up transients, we found oscillations in the particle velocities (data not shown) at 0.1 Hz (slow flow) to 1 Hz (fast flow). This feature, which we discuss elsewhere, is ubiquitous in the pipe flow of pastes [5,18]. Here, we restrict ourselves to steady-state velocity profiles, $\langle V \rangle$, obtained by averaging over 20 s (slow flow) to 10 s (fast flow), corresponding to ~2000 and to ~1000 frames, respectively. We imaged at $x \sim 0.5$ cm from the entrance to the capillary (corresponding to ~2000 particles), where entry effects have died out and the results show negligible x dependence.

Typical data for smooth walls are shown in Fig. 1. For $z \gtrsim 10$ μm, each velocity profile consists of a shear zone close to the walls and a nearly unsheared central ''plug.''

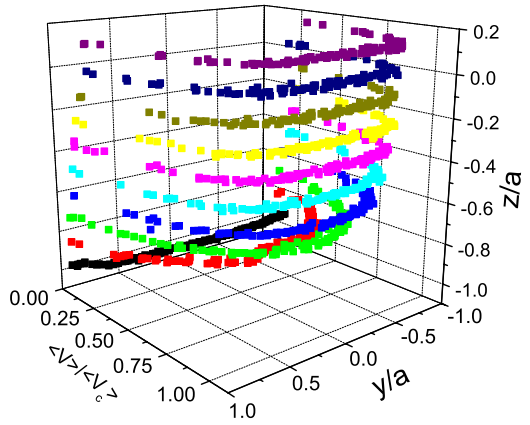

FIG. 1 (color online). Velocity profiles in the lower half of the capillary (width $2a = 50\ \mu$m) with smooth walls reconstructed in 3 μm steps. The average velocity $\langle V \rangle$ is in units of the average velocity of the central, unsheared, plug, $\langle V_c \rangle = 20\ \mu\text{m s}^{-1}$.

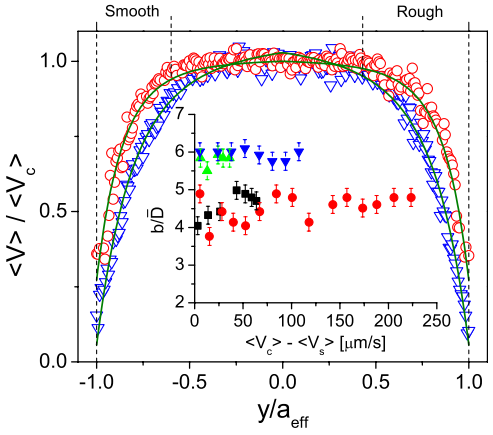

FIG. 2 (color online). Averaged velocity profile as a function of y/a_{eff} for smooth (red, ○) and rough (blue, ▽) walls at $z = 17\ \mu$m. Full lines: fits from integrating Eq. (7); dotted lines: extents of sheared zones. $\langle V_c \rangle$ is 114 $\mu\text{m s}^{-1}$ (80 $\mu\text{m s}^{-1}$) for smooth (rough) walls. Inset: b in units of particle diameter as a function of ΔV. Green, ▲ and blue, ▼: two runs for rough walls; red, ● and ■: two runs for smooth walls.

This plug shrinks at smaller z, i.e., closer to the bottom wall. We also observe wall slip with velocity $\langle V_s \rangle$. The profiles for smooth and rough walls, Fig. 2, are qualitatively similar, but the latter displays considerably smaller wall slip and larger shear zones. Wall slip only constitutes a small fraction of the flow within the material: $\langle V_s \rangle / \langle V_c \rangle \lesssim 15\%$ (30%) for rough (smooth) walls. Note that for rough walls, we use an effective half-width $a_{\text{eff}} = a - \bar{D}_{\text{coat}} - \bar{D}/2$; for smooth walls, $a_{\text{eff}} = a - \bar{D}/2$. Finally we exclude any inertia effects given that typical Reynolds numbers $\lesssim 10^{-6}$.

The dependence of the velocity profiles on the overall flow rate is striking. Define the width of the shear zone b as the distance from the wall where the flow speed is $\langle V_s \rangle + 0.95\Delta V$, where $\Delta V = \langle V_c \rangle - \langle V_s \rangle$ is the difference between the averaged center and wall speeds (with $\Delta V/a$ the average shear rate) [19]. We see (inset Fig. 2) that b is independent of ΔV; i.e., the central plug remains essentially constant for flow rates varying by more than one decade. More strongly, the normalized velocity profiles $(\langle V \rangle - \langle V_s \rangle)/\Delta V$ for different flow rates collapse onto two master curves for rough and smooth walls, Fig. 3.

Let us now compare the observed behavior to what is expected from bulk rheology. Concentrated PMMA suspensions ($\phi > 0.58$) behave as glassy yield-stress fluids, with stress τ versus strain rate $\dot{\gamma}$ relation $\tau - \tau_{\text{yield}} \propto \dot{\gamma}^n$ [Herschel-Bulkley (HB) fluids], with τ_{yield} the yield stress and $n \approx 0.5$ [6]. Plug flow is ubiquitous in all yield-stress fluids, and has been extensively studied [20]. Thus, our observation of plug flow is, in itself, unsurprising. In yield-stress fluids, if the maximum applied shear stress in the channel exceeds τ_{yield}, we have plug flow with shear zones whose boundaries are given by $\tau = \tau_{\text{yield}}$; hence, the width of the shear zone, b, grows with the shear rate and eventually leaves a vanishingly small plug [20]. Extracting rheological properties from [6], we can predict how our system should behave as an HB fluid. The relevant parameter is the ratio of yield to viscous stress, the Oldroyd number (Od). We estimate that in our experiments, Od $\lesssim$ 0.02 for all flow speeds. From [20], this corresponds to complete yielding throughout the channel at all values of ΔV. This is not what we observe.

A clue to what may be happening in our experiments comes from observing that at the typical strain rate encountered in the shear zones, $\tau_B(\Delta V/a) \sim 50$, conventional rheology would lead us to expect severe shear thickening. Shear thickening in pastes is very far from fully understood on the microscopic level [8,21,22], but we may speculate that for colloids stabilized by short grafted polymers, interparticle friction may become important as they jam against each other driven by shear. Indeed, the measured transverse fluctuations of particles clearly show the mo-

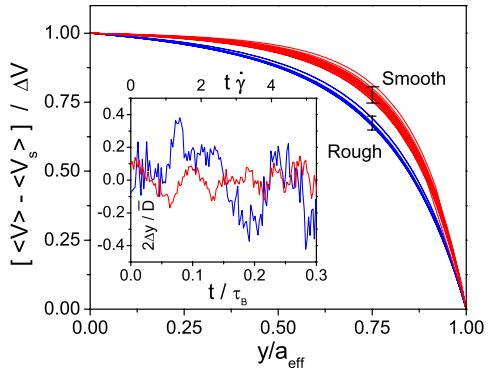

FIG. 3 (color online). Normalized velocity profiles at $z = 17\ \mu$m versus y/a_{eff}. We use the profiles fitted from integrating Eq. (7); the error bars show the spread in the measured data. Inset: normalized transverse fluctuations of particles in the shear zone for the two boundary conditions, versus normalized time t/τ_B or *local* accumulated strain $t\partial\langle V(y)\rangle/\partial y = t\dot{\gamma}(y)$, top axis. The traces show larger fluctuations for rough walls.

tions induced by them "bumping" along neighboring layers, Fig. 3 inset. We are thus led to consider analogies with friction-dominated granular flow.

Indeed, both the width of the shear zone $b \sim 6\bar{D}$ ($\sim 5\bar{D}$ for smooth walls) and the lack of flow rate dependence, are strongly reminiscent of observations in gravity-driven "chute flow" of dry granular materials [23]. In particular, Pouliquen and Gutfraind observed $b \approx 6D$ in the two-dimensional flow of discs (diameter D) for channels of widths $10D \leq 2a \leq 44D$ and developed a model to account for their observations [23,24]. Below, we extend their model to three dimensions, and show that it indeed predicts b independent of ΔV.

Following [23] we start with the components of the stress tensor $\boldsymbol{\tau}$ in the fully developed flow of a continuum medium in the x direction along a pipe, which satisfies

$$\frac{\partial \tau_{xx}}{\partial x} + \frac{\partial \tau_{xy}}{\partial y} + \frac{\partial \tau_{xz}}{\partial z} = 0, \tag{1}$$

$$\frac{\partial \tau_{yy}}{\partial y} = \frac{\partial \tau_{zz}}{\partial z} = 0, \tag{2}$$

with $\partial \tau_{xx}/\partial x = -\nabla p$. For a square pipe of side $2a$ [25]:

$$\tau_{xy}(z) = \tau_0 \sum_{k=1,3,5\ldots}^{\infty} (-1)^{(k+1)/2} \times \left[1 - \frac{\cosh(k\pi z/2a)}{\cosh(k\pi/2)}\right] \frac{\sin(k\pi y/2a)}{k^2}, \tag{3}$$

where $\tau_0 = 8a\nabla p/\pi^2$. This constant sets the scale for the (z-dependent) maximum stress at the wall, $\tau_{\max}$.

To determine the normal stress, τ_{yy} we impose a Coulomb friction condition at the walls:

$$\tau_{yy} = \mu_{\text{wall}}^{-1} \tau_{\max}, \tag{4}$$

where μ_{wall} is the friction coefficient between the suspended particles and the wall; this constant τ_{yy} satisfies Eq. (2) [26]. Following the Coulomb criterion, the material yields if $\tau_{xy} \geq \tau_{\text{yield}} \equiv \mu_{\text{bulk}} \tau_{yy}$, with μ_{bulk} the friction coefficient inside the material. We expect $\mu_{\text{wall}} \leq \mu_{\text{bulk}}$, with "=" for a rough wall coated with particles, and "<" for smooth, glass walls. From Eq. (4) we have

$$\tau_{\text{yield}} = (\mu_{\text{bulk}}/\mu_{\text{wall}})\tau_{\max} \geq \tau_{\max}. \tag{5}$$

Since $\tau_{xy} \leq \tau_{\text{yield}}$, the bulk never yields and the whole material slips as a plug. Note from Eq. (5) that τ_{yield} increases with $\tau_{\max}$ (and therefore ΔV). This reflects the rising normal stress τ_{yy}, Eq. (4), which increases the friction between particles and thus τ_{yield} [27].

We now assume the presence of stress fluctuations which, when added to the continuum τ_{xy}, Eq. (3), may take the local stress above τ_{yield}, Fig. 4. Following [23] we use a "Boltzmann" ansatz for the yielding probability,

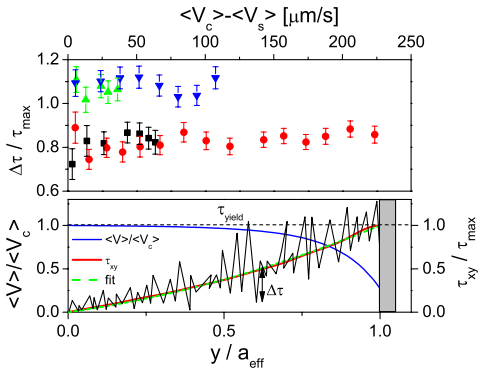

FIG. 4 (color online). (Top) Fitted fluctuating stress amplitude $\Delta\tau$ in units of $\tau_{\max}$ as a function of the "net shear", ΔV; symbols as in Fig. 2. (Bottom) Schematic of the fluctuating shear stress superimposed on the continuum τ_{xy}. The dashed line shows the quadratic fit used for the integration.

$$p_{\text{yield}} \propto \exp\left[-\frac{\tau_{\text{yield}}(z) - |\,\tau_{xy}(y,z)\,|}{\Delta\tau}\right], \tag{6}$$

where $\Delta\tau \equiv \Delta\tau(z)$ is the amplitude of the τ_{xy} fluctuations, taken to be independent of y at any particular z. The model is completed by the simplest possible ansatz relating shear rate to p_{yield}: $\partial V(y,z)/\partial y \propto p_{\text{yield}}$ [28]. At a fixed $z = z_0$, therefore, we have

$$\frac{\partial V(y,z_0)}{\partial y} = \text{const} \times \exp\left[\frac{\tau_{xy}(y,z_0)}{\Delta\tau}\right]. \tag{7}$$

In order to perform the integration analytically we fitted the stress profile, Eq. (3), with a quadratic approximation; Fig. 4 (bottom) shows both the analytic expression and the fit. We then substituted the fitted stress into Eq. (7), integrated and fitted the resulting velocity profile to the measured data. Example results are shown in Fig. 2.

The fitted stress fluctuation amplitudes normalized to the wall stress, $\Delta\tau/\tau_{\max}$, at $z = 17$ μm for both smooth and rough walls are plotted against ΔV in Fig. 4. As $\tau_{\max}$ increases with flow rate, $\Delta\tau$ increases proportionally so that their ratio remains constant. Combined with Eqs. (3) and (5) this means that $(\tau_{\text{yield}} - |\tau_{xy}|)/\Delta\tau$ in Eq. (6) is independent of $\tau_{\max}$, resulting in a constant value for b, Fig. 2, and collapse of the velocity profiles, Fig. 3.

The fact that $\Delta\tau$ scales as the wall stress $\tau_{\max}$ suggests that the stress fluctuations are controlled by what happens at the boundaries. Two-dimensional simulations of dry granular matter indeed relate stress fluctuations to inhomogeneities in the friction-dominated force chains resulting from contacts at the walls [29]. Here, we find (for $z \sim a$) that $\Delta\tau/\tau_{\max}$ for rough walls is somewhat larger than for smooth walls, Fig. 4; this difference is directly correlated with the observed difference in b, Fig. 2. The presence of such a difference, and its sign, is unsurprising. Flow along a smooth wall is less "bumpy" and can thus be expected to generate a lower level of stress fluctuations

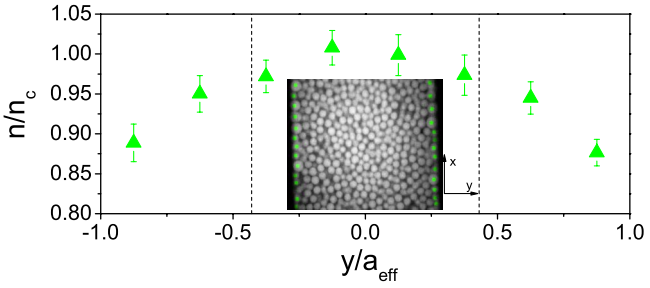

FIG. 5 (color online). Average density profile at $z = 17$ μm for rough walls, in units of the density n_c in the center. Dashed lines: $\pm b$ for rough walls. Inset: corresponding confocal micrograph; the particles marked with ● are attached to the walls.

which propagate through the system, as also shown by the two traces in the inset to Fig. 3 [30].

The analogy with granular flow extends further than the constant shear zone width. In [23], a variation of the density across the channel was observed, the plug being $\sim$10% denser than the edge of the shear zone. We observe the same feature in our flows. Figure 5 shows a typical density profile at $z = 17$ μm, measured by counting particles per unit area and averaging 10^4 frames; this profile is independent of the overall flow rate. The observed density reduction in the shear zone is not unexpected, since dilatancy is required in flowing particulates (dry or wet) at such high packing fractions. Analogous density profiles are found in smooth walls channels.

Our findings also have implications concerning the role played by confinement. Since $\bar{D}/2a \approx 20$, one might expect some size dependence. However, the width of the shear zone b we observed is always smaller than the half-width of the channel, a, and size effects should only become dominant for channels with $a \lesssim b$.

To summarize, we have measured the flow properties of a nearly random close-packed hard-sphere colloid driven by a constant pressure gradient in a 20-particle-diameter square channel by tracking the motion of individual particles using fast confocal microscopy. At all flow rates, we observed a central, almost unsheared plug, and peripheral shear zones. The observed size of the shear zone contrasted with the prediction for an ideal yield-stress fluid and remained constant as the flow rate was increased. We explained this by appealing to a model originally set up for the gravity-driven ''chute flow'' of dry granular materials [23]. This model should be applicable in our case if the yield stress, τ_{yield}, is dominated by interparticle friction. The model predicts that stress fluctuations can bring about yielding even when the average stress is below τ_{yield}. Quantitative velocity fits to our data were obtained. Furthermore, our approach applied to a Couette geometry fits well the velocity profiles for wet grains measured in [31], although it leaves open the reason for the flow-dependent b at low speeds observed in that work. Finally, we expect a transition back to a conventional, non frictional regime when the time scales of Brownian motion become comparable to the ones set by the shear flow. The crossover will be strongly dependent on volume fraction, but preliminary measurements show that, surprisingly, friction still dominates down to $\phi = 0.56$ for the range of ΔV studied here.

We thank Andrew Schofield for providing the particles and Eric Weeks and Alexander Morozov for helpful discussions. L. Isa was funded by the EU network No. MRTN-CT-2003-504712, and R. Besseling by EPSRC No. GR/S10377/01 and No. EP/D067650/1.

[1] R. G. Larson, *The Structure and Rheology of Complex Fluids* (Oxford University, Oxford, 1999).
[2] J. Bent *et al.*, Science **301**, 1691 (2003).
[3] J. A. Lewis, J. Am. Ceram. Soc. **83**, 2341 (2000).
[4] D. I. Wilson *et al.*, Chem. Eng. Sci. **61**, 4147 (2006).
[5] M. D. Haw, Phys. Rev. Lett. **92**, 185506 (2004).
[6] G. Petekidis *et al.*, J. Phys. Condens. Matter **16**, S3955 (2004).
[7] K. N. Pham *et al.*, Europhys. Lett. **75**, 624 (2006).
[8] W. J. Frith *et al.*, J. Rheol. (N.Y.) **40**, 531 (1996).
[9] D. Lootens *et al.*, Phys. Rev. Lett. **90**, 178301 (2003).
[10] D. Psaltis *et al.*, Nature (London) **442**, 381 (2006).
[11] M. Fuchs and M. E. Cates, Phys. Rev. Lett. **89**, 248304 (2002).
[12] C. S. Campbell, Powder Technol. **162**, 208 (2006).
[13] G. D. R. MiDi, Eur. Phys. J. E **14**, 341 (2004).
[14] L. Isa *et al.*, J. Phys.: Conf. Ser. **40**, 124 (2006).
[15] J. C. Crocker and D. G. Grier, J. Colloid Interface Sci. **179**, 298 (1996).
[16] Applying this to the flow of a 30% suspension in a 2D channel gave parabolic profiles [14] as also found in [17].
[17] M. Frank, J. Fluid Mech. **493**, 363 (2003).
[18] P. Yaras *et al.*, Rheol. Acta **33**, 48 (1994).
[19] This corresponds to the point where noise in the raw data makes it impossible to detect any curvature in the profiles.
[20] R. R. Huilgol and Z. You, J. Non-Newtonian Fluid Mech. **128**, 126 (2005).
[21] M. E. Cates *et al.*, Phys. Rev. Lett. **81**, 1841 (1998).
[22] R. C. Ball and J. R. Melrose, Adv. Colloid Interface Sci. **59**, 19 (1995).
[23] O. Pouliquen and R. Gutfraind, Phys. Rev. E **53**, 552 (1996).
[24] O. Pouliquen, Phys. Rev. Lett. **93**, 248001 (2004).
[25] F. M. White, *Viscous Fluid Flow* (McGraw-Hill, New York, 1991), 2nd ed.
[26] A completely analogous discussion can be given for τ_{zz} and τ_{zz} leading to a velocity profile $V(z)$.
[27] Thus, this *variable* Coulombic yield stress is not the same as the *constant* yield stress in, say, the HB model.
[28] The ansatz 6 was proposed [23] to account for shear-zone behavior next to walls, and is qualitatively incorrect for the center of the pipe, where we must have $\partial V/\partial_y = 0$.
[29] R. Gutfraind and O. Pouliquen, Mech. Mater. **24**, 273 (1996).
[30] We also note that for smooth walls we find considerable layering in the structure close to the walls [14].
[31] N. Huang *et al.*, Phys. Rev. Lett. **94**, 028301 (2005).